

Study of series resonance overvoltage at LV side of transmission transformer during EHV cable energization

F. Barakou, A. Pitsaris, P.A.A.F. Wouters, E.F. Steennis

Abstract—A series resonance between the leakage transformer inductance and HV cable capacitance can be excited by a voltage disturbance at the EHV side of the transformer. In this paper, the series resonance phenomenon is initially studied using lumped parameters to analytically obtain the resonance frequencies and estimate how each parameter affects the first series resonance as well as the harmonic content of the cable energization. For the load impedance two different configurations, consuming the same active and reactive power, are tested: parallel RL load and series RL load. It is concluded that the type of load model greatly affects the harmonic impedance of the system leading to different resonance behavior. The effect of the secondary circuit consisting of the transformer, the HV cable and the load is also investigated and is shown that it significantly affects the frequency of the harmonic content produced during EHV cable energization. In addition, the accuracy of the analytical formulas is assessed by modeling the basic circuit in PSCAD/EMTDC using the frequency-dependent phase model for cable and OHL modeling.

Keywords: power transmission, power system simulation, power system transients, series resonance, underground power cables, PSCAD/EMTDC

I. INTRODUCTION

IN recent years there is an increase in the use of Extra High Voltage (EHV) underground cables (UGC) in transmission networks. Although this development is quite encouraging from a societal perspective, new challenges may arise from a technical perspective. More specifically, the electrical characteristics of cables differ significantly from overhead lines (OHLs) mainly due to the higher capacitance which can shift the harmonic impedance of the network to lower frequencies and lead to temporary overvoltages (TOV) due to resonance [1]. In this paper the series resonance involving leakage transformer inductance and HV cable capacitance is investigated.

A series resonance study was performed also in [2] with the difference that the high-Frequency interaction was of interest where the voltage ratio between the two transformer windings is significantly increased for frequencies above 100 kHz. The

This work was financially supported by TenneT TSO B.V. within the framework of the Randstad380 cable research project, Arnhem, the Netherlands.

F. Barakou, A. Pitsaris, P.A.A.F. Wouters and E.F. Steennis are with the Electrical Energy Systems group, Department of Electrical Engineering, Eindhoven University of Technology, P.O.Box 513, 5600 MB Eindhoven, the Netherlands (email of corresponding author: f.barakou@tue.nl)

E.F. Steennis is also with DNV-GL Energy, P.O.Box 9035, 6800 ET Arnhem, the Netherlands

Paper submitted to the International Conference on Power Systems Transients (IPST2017) in Seoul, Republic of Korea June 26-29, 2017

emphasis of this paper is the low-frequency series resonance. In a transmission network the leakage inductance of a transformer can create a series resonant circuit with the capacitance of a cable. When excited by a voltage disturbance of its natural frequency, it will draw a significant amount of current creating an overvoltage at the secondary side of the transformer [3]–[5]. A voltage disturbance can arise when energizing an EHV power cable and due to the high cable capacitance the harmonic content of the energization can shift to very low frequencies, causing a TOV due to the low damping at such frequencies. The most important parameters that need to be

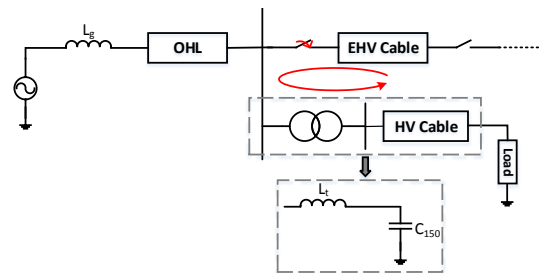


Fig. 1. Series resonance configuration.

determined for such kind of studies are the natural frequency of the secondary circuit consisting of transformer, HV cable and load as well as the frequency of the voltage harmonic components during the energization of the EHV cable.

The natural frequency of the secondary circuit can be determined using frequency scans or even by using simple analytical expressions. However, the frequency of the voltage harmonic components during EHV cable energization is much more difficult to be found without using time domain simulations since there are many parameters that affect its value. In [6]–[8] the authors derive theoretical formulas and calculation methods for the frequency component contained in the energization overvoltage of both cable and OHL responses. In those cases the effect of the source impedance and possible load connected at the receiving end of the EHV UGC/OHL were taken into account, however the effect of the secondary circuit comprising the transformer and HV cable was not considered.

II. DERIVATION OF ANALYTICAL EXPRESSIONS

In order to estimate how each parameter affects the first series resonance as well as the harmonic content of the cable

energization the simplified network of Fig. 1 is used where for the OHL and cables the single Pi model is utilized, the transformer is modeled only by its leakage inductance and the load comprises of an RL circuit. In order to derive simple analytical expressions the mutual coupling between phases is not taken into account and each component is expressed using the ABCD matrix formalism. The configuration of Fig. 1 can be represented as shown in Fig. 2 (see Appendix A).

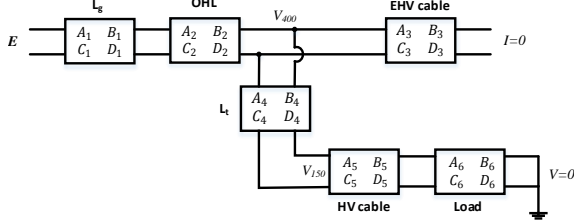


Fig. 2. ABCD matrix connection.

The harmonic content of the energization at the EHV side, i.e. 400 kV, is given by:

$$\frac{V_{400}}{E} = \underbrace{[B_7^{-1}A_7 + C_3A_3^{-1} + D_8B_8^{-1}]^{-1}}_{G_1} \cdot B_7^{-1} \quad (1)$$

while in the HV side, i.e. 150 kV:

$$\frac{V_{150}}{E} = A_4^{-1} \cdot [G_1 - B_4D_9B_8^{-1}G_1] \quad (2)$$

The resulting expressions of equations (1) and (2) are complex functions and in order to find the dominant frequencies of energization their absolute values are used and the frequencies of the local maxima are calculated.

In order to calculate the harmonic impedance at EHV side the source is short-circuited ($E=0$) and a current source (I_H) is assumed to be connected at the point of interest. From nodal equation at this point the impedance is found as:

$$\frac{V_{400}}{I_H} = [B_7^{-1}A_7 + C_3A_3^{-1} + D_8B_8^{-1}]^{-1} \quad (3)$$

The expressions of the ABCD parameters 7, 8 and 9 can be found in Appendix A.

A. Effect of load model

If there is no load connected to the HV cable then the natural frequency is given as:

$$f_n = \frac{1}{2\pi\sqrt{L_t C_{150}}} \quad (4)$$

where L_t is the leakage inductance of the transformer and C_{150} is the capacitance of the HV cable. In order to introduce damping and make the series resonance study more realistic a load is connected at the receiving end of the HV cable and in this case the natural frequencies are given by the roots of equation:

$$\rho_4 \omega^4 - \rho_2 \omega^2 + \rho_0 = 0 \quad (5)$$

This equation will result in two positive frequencies, and the higher one is the series resonant frequency. The values of

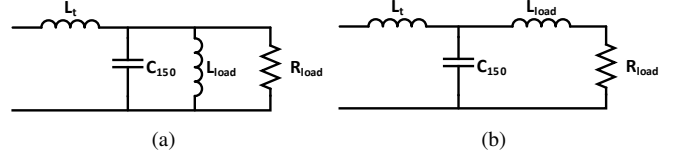


Fig. 3. Series resonant circuit with (a) parallel load model and (b) series load model.

ρ_0 , ρ_2 and ρ_4 depend on the type of load model used.

For parallel load model (Fig. 3a) the expression becomes:

$$\begin{aligned} \rho_4 &= C_{150}L_tL_{load}^2R_{load}^2 \\ \rho_2 &= 2C_{150}L_tL_{load}R_{load}^2 + C_{150}L_{load}^2R_{load}^2 - L_tL_{load} \\ \rho_0 &= (L_t + L_{load})R_{load}^2 \end{aligned}$$

For the series load (Fig. 3b) the expression becomes:

$$\begin{aligned} \rho_4 &= C_{150}^2L_tL_{load}^2 \\ \rho_2 &= -C_{150}^2L_tR_{load}^2 + 2C_{150}L_tL_{load} + C_{150}L_{load}^2 \\ \rho_0 &= -C_{150}R_{load}^2 + L_t + L_{load} \end{aligned}$$

The resistance and reactance of these two load models are calculated as in [9] depending on the demand of active and reactive power. However, the resonant behavior between them presents major differences even for the same active and reactive power demand. For a base loading condition of 100 MW + j50 MVar and the same transformer leakage inductance the harmonic impedance comparison of only the secondary circuit is depicted in Fig 4a. The network parameter values can be found in Appendix B. For the parallel load case the series resonance is more damped, since the magnitude of the impedance at the resonance frequency is much larger than in the series load case. In Fig. 4b the harmonic impedance comparison of the complete circuit of Fig. 1, measured at the EHV side for the two load models is illustrated where the damping is much higher in the parallel load case and the series resonance cannot be identified as in the series load case (zoomed-in part). Moreover, there is an obvious difference in the amplification ratio between EHV and HV (see Fig. 4c) whereas for the parallel load case even at the series resonance frequency almost no amplification is present.

Thus, one must be cautious for the choice of load model when conducting a series resonance study. From the analysis it can be observed that the parallel load model provides excessive damping and it is almost impossible to identify series resonance cases even in a simple network. Thus for the rest of the sensitivity analysis the series load model will be used.

B. Effect of 150 kV cable length

For conducting a series resonance study the steps that need to be followed are described in [3] and [5] where by using time domain simulations the dominant harmonic components contained in the EHV cable energization are found as well as the voltage amplification ratio from EHV to HV. Next, to have a series resonance the natural frequency of the secondary

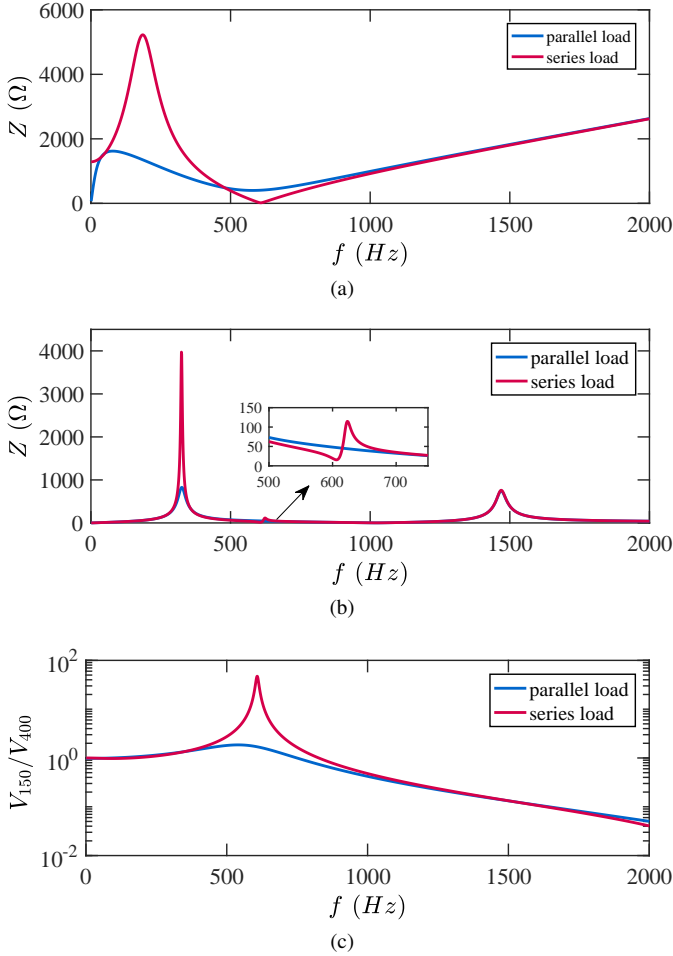


Fig. 4. Comparison of (a) the harmonic impedance of the series resonant circuit, (b) the harmonic impedance of the full circuit and (c) the amplification ratio between EHV and HV for two load model types.

circuit is adjusted (by changing the HV cable capacitance) in order to match the harmonic component of the energization. Then time domain simulations are again conducted to assess the severity of the resonance overvoltage. However, by using this method it is not taken into account that by changing the HV cable capacitance the harmonic content of the energization is also changing. To show this effect, using (1) and (2) the length of the HV cable is increased from 5 km to 50 km with a step of 1 km while the rest of the network parameters are constant. The base case of the network parameters can be found in Appendix B.

It can be seen from Fig. 5a that when the length of the 150 kV cable is 5 km the dominant energization frequency is 330 Hz while the series resonance frequency is 866 Hz (the second energization frequency is almost the same as the series resonance but the amplitude is very low). If the method described above is followed then the length of the 150 kV cable is adjusted in order for the series resonance frequency to become 330 Hz and that is succeeded for 32 km of cable. However, for 32 km of 150 kV cable the dominant energization frequencies are changed to 278 Hz and 394 Hz. As can be

seen in Fig. 5b the amplification ratio at these frequencies is much lower than the actual series resonance frequency. The

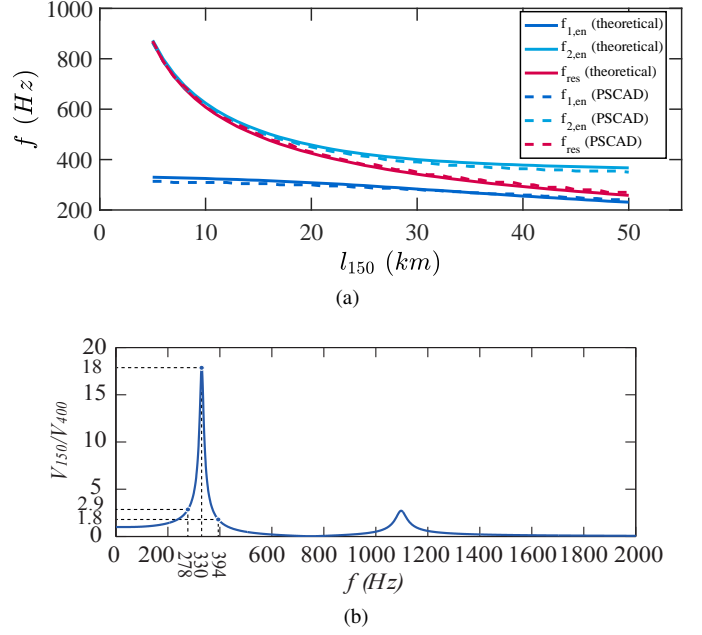


Fig. 5. (a) Energization frequencies and series resonance as function of 150 kV cable length, where the continuous lines are obtained from the theoretical expressions while the dashed lines from PSCAD simulations and (b) amplification ratio for 32 km cable length and 0.217 H transformer inductance.

frequencies obtained from the theoretical expressions are also compared with the ones calculated by time domain simulations where both cables and OHL were modeled using the Frequency-Dependent Phase model including cross-bondings for the 400 kV cable. Minor deviations are observed between the two, verifying the validity of the approximate expressions.

From the above analysis it can be concluded that the length of the 150 kV cable affect both the frequency of the series resonance and the harmonic content of the energization making it more complex to intentionally assess a series resonance case.

III. PARAMETRIC ANALYSIS

Even though the theoretical expressions provide a quick way to estimate the frequencies of the energization harmonic content as well as the amplification ratio between HV and EHV busbars it is not clear how these values are translated in time domain and more specifically the maximum resonance overvoltage. In order to identify how each network parameter affect the maximum overvoltage a parametric analysis is conducted using the PSCAD/EMTDC software.

In Fig. 6 the variation of the maximum overvoltage at the 150 kV side is depicted for four different transformer inductances and three 400 kV cable lengths. The length of the 150 kV cable is increased from 5 km to 80 km with a step of 1 km, which means that in total 912 simulation cases were run. Usually, such extensive parametric analysis is very difficult to be conducted in EMT type software but in

this case the new automation feature of interfacing PSCAD with Python 3.5 was used and the change of the multiple parameters were realised using nested loops and no manual change was required. It can be seen from Fig. 6 that for low

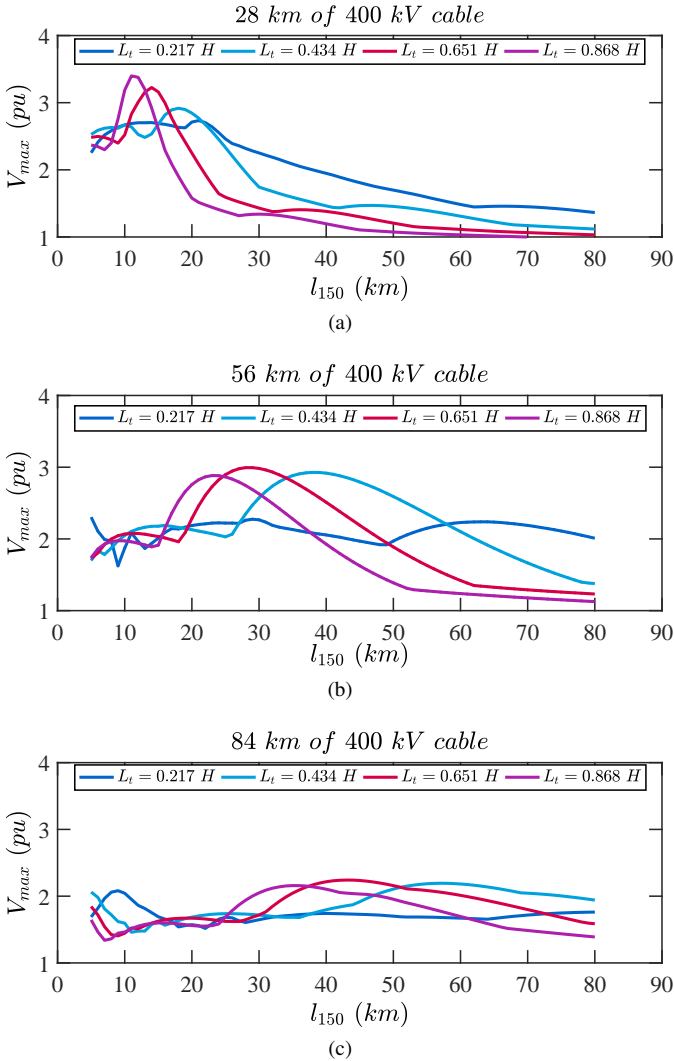


Fig. 6. Maximum overvoltage variation at the 150 kV side for four different transformer inductances as function of the length of the 150 kV cable for (a) 28 km of 400 kV cable (b) 56 km of 400 kV cable and (c) 84 km of 400 kV cable.

transformer inductance no clear resonance peak for a certain range of 150 kV cable length is present. Moreover, for all four transformer inductance cases, as the length of the 400 kV cable increases, the maximum resonant overvoltage decreases and its width increases. Furthermore, while in Fig. 6a the increase of transformer inductance causes an increase in the maximum overvoltage for larger 400 kV cable lengths the last increase of the inductance value causes a decrease in the maximum overvoltage (see Fig. 6b and Fig. 6c).

The time domain waveforms of the voltages observed at the 150 kV busbar for the lowest and highest transformer inductances of Fig. 6a are shown in Fig. 7. It is clear that as the transformer inductance increases (and consequently the length

of the 150 kV cable that gives rise to a resonance decreases) more severe series resonance is caused.

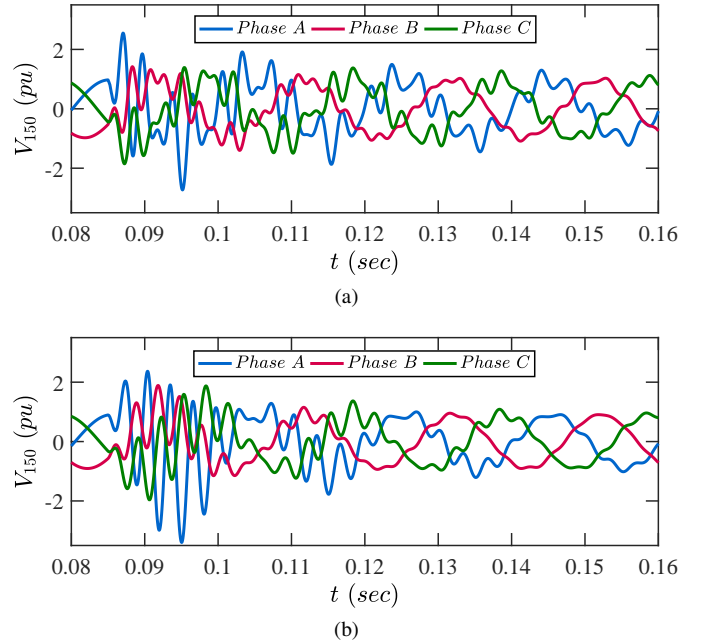


Fig. 7. Voltage waveforms at the 150 kV side for 28 km of 400 kV cable and for transformer inductance (a) 0.217 H (b) 0.868 H.

This can be attributed to the fact that when the transformer inductance is higher, smaller HV cable length is needed to achieve the series resonance and the energization dominant frequencies are closer to the series resonance frequency. An example is illustrated in Fig. 8 for a transformer inductance of 0.868 H. For 11 km of HV cable (the length where the maximum overvoltage occur according to Fig. 6a) the dominant energization frequencies at 304 Hz and 359 Hz are much closer to the series resonance frequency of 331 Hz compared to those shown in Fig. 5. Moreover, the amplification ratio for 11 km HV cable (see Fig. 8b) at these two frequencies is much higher than the one in Fig. 5b. However, the increase in the transformer inductance results in a decrease of the amplification ratio peak at the resonant frequency. Thus there is a trade-off when increasing the transformer inductance between the closer the dominant frequencies get to the series resonance frequency and the decrease in the amplification ratio at the series resonance frequency.

IV. STUDY ON DUTCH 380 kV GRID

The Dutch TSO, TenneT, has integrated a 10.8 km cable connection between two substations (Wateringen and Bleiswijk) in a mixed OHL-UGC double circuit connection [10]. For this series resonance study one of the possible worst case scenarios is examined, where one EHV circuit is energized (from Bleiswijk side) while the other circuit is out of service. Further, only one of the three transformers at this substation is in service and only one of the two 150 kV cables (of 17 km) is in operation. For this study the whole Dutch 380 kV network has been modeled and the type of modeling of

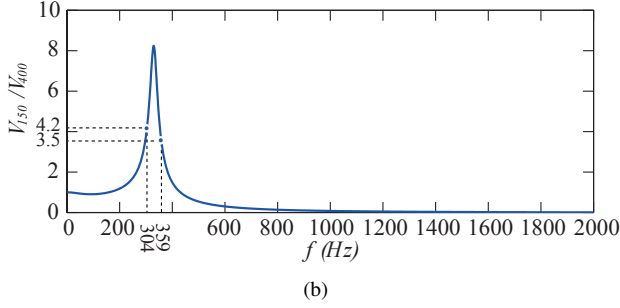
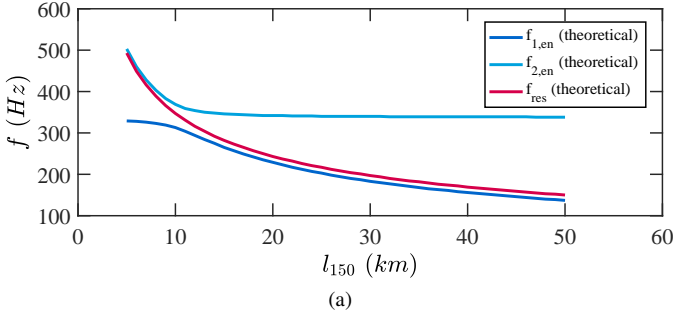


Fig. 8. (a) Energization frequencies and series resonance as function of 150 kV cable length and (b) amplification ratio for 11 km cable length for 0.868 H transformer inductance.

each component can be found in [5], [10]–[15]. The simulation model was validated through dedicated transient measurements upon cable energization, the results of which will be presented in a follow-up paper.

A. Results

First the harmonic impedance of the series resonant circuit (transformer-cable-load) was calculated using frequency scan and the series resonance frequency was found to be 468 Hz. Connecting the secondary circuit the energization case is run and as can be seen in Fig. 9 there is a clear amplification of the energization harmonic content from EHV to HV at 410 Hz and 500 Hz since the dominant frequencies are relatively close to the series resonance. From the time domain waveforms of Fig. 10 it is observed that the maximum overvoltage of 1.4 pu at 400 kV becomes 1.8 pu at 150 kV, but it is still much lower than the switching impulse withstand voltage and since the oscillations are quickly damped the severity of the series resonance at this point under the specific conditions is low.

Moreover, the case of a larger 150 kV cable (22 km) was examined in order for the series resonance to match the 410 Hz of the dominant energization frequency. Also in this case no severe series resonance was observed and the maximum overvoltage at 150 kV was even lower (1.7 pu). This can be attributed to the fact that the leakage inductance of the transmission transformer is low and the case of Fig. 5a is observed where the energization frequencies shift significantly with the increase of the 150 kV cable length.

V. CONCLUSIONS

This paper investigates the phenomenon of series resonance between the transmission transformer inductance and

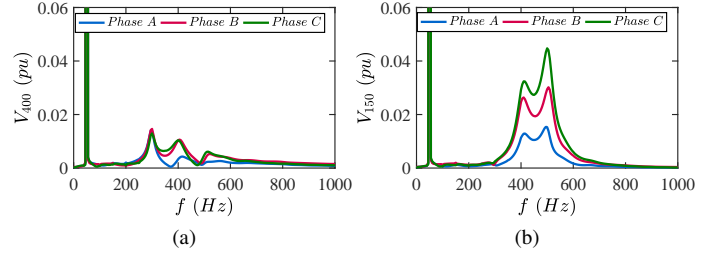


Fig. 9. FFT transform on (a) 400 kV and (b) 150 kV voltage waveform upon energization

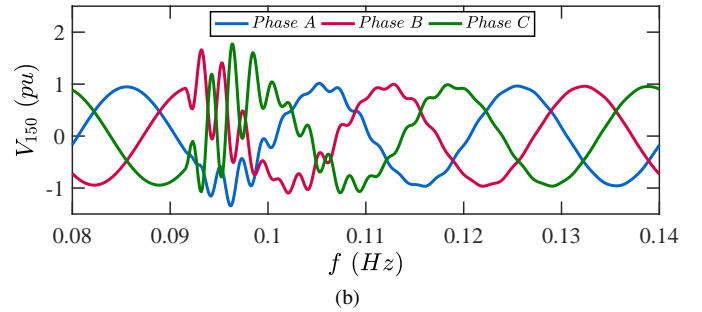
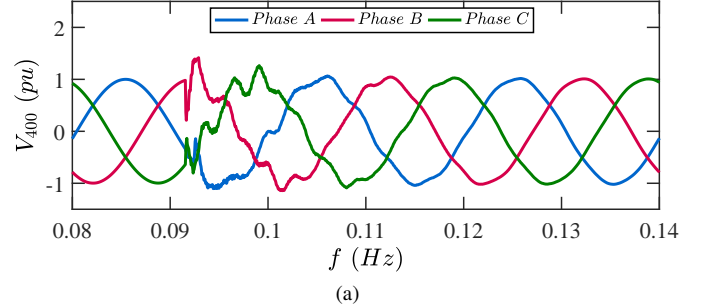


Fig. 10. Voltage waveforms at (a) 400 kV and (b) 150 kV side of the transformer upon energization.

HV cable capacitance due to EHV cable energization. First approximate expressions using lumped parameter models for the network components were developed in order to quickly assess the harmonic impedance of the network and the dominant energization frequencies. Their resulting frequencies were compared with the ones calculated from time domain simulations and the deviation was small verifying that they can be an accurate enough quick way to assess the energization dominant frequencies.

An addition to previous series resonance studies is related to the investigation of the effect of the load and 150 kV cable length on the series resonance damping and frequencies. It can be concluded that the load model (series or parallel) has a dominant effect on the resonance damping whereas the variation in 150 kV cable length shifts the harmonic frequencies of energization.

Another contribution of this study, resulted from the parametric analysis, is that the transformer inductance has a major effect on the severity of the series resonance where for very low transformer inductances there is practically no dominant

resonance overvoltage.

From the Dutch grid case study it can be concluded that under the specific conditions no severe series resonance case is caused by EHV cable energization, even when the 150 kV cable is adjusted to match the dominant energization frequency. This can be mainly attributed to the low leakage inductance of the transformer.

APPENDIX A

The external network and transformer were modeled as a single inductance so:

$$\begin{bmatrix} A_{1,4} & B_{1,4} \\ C_{1,4} & D_{1,4} \end{bmatrix} = \begin{bmatrix} 1 & sL_{g,t} \\ 0 & 1 \end{bmatrix} \quad (6)$$

For the OHL the pi model was used thus the three matrices have the form:

$$\begin{bmatrix} A_2 & B_2 \\ C_2 & D_2 \end{bmatrix} = \begin{bmatrix} 1 + ZY & Z \\ (2 + ZY)Y & 1 + ZY \end{bmatrix} \quad (7)$$

where $Z = l \cdot (R + sL)$, $Y = l \cdot s\frac{C}{2}$ and l is the length of the line.

The same holds for both cable connections only in this case shunt reactors are connected at the sending and receiving end of the cable in order to achieve 100% compensation.

$$\begin{bmatrix} A_{3,5} & B_{3,5} \\ C_{3,5} & D_{3,5} \end{bmatrix} = \begin{bmatrix} 1 & 0 \\ \frac{1}{sL_c} & 1 \end{bmatrix} \cdot \begin{bmatrix} 1 + ZY & Z \\ (2 + ZY)Y & 1 + ZY \end{bmatrix} \cdot \begin{bmatrix} 1 & 0 \\ \frac{1}{sL_c} & 1 \end{bmatrix} \quad (8)$$

where $L_c = \frac{2}{\omega^2 C}$ computed at the nominal frequency.

The load was also modeled as a series impedance where the output voltage is zero (grounded):

$$\begin{bmatrix} A_6 & B_6 \\ C_6 & D_6 \end{bmatrix} = \begin{bmatrix} 1 & Z \\ 0 & 1 \end{bmatrix} \quad (9)$$

where for the series load model $Z = R_l + sL_l$ while for the parallel load $Z = \frac{R_l \cdot sL_l}{R_l + sL_l}$.

Moreover the following ABCD matrices are defined:

$$\begin{bmatrix} A_7 & B_7 \\ C_7 & D_7 \end{bmatrix} = \begin{bmatrix} A_1 & B_1 \\ C_1 & D_1 \end{bmatrix} \cdot \begin{bmatrix} A_2 & B_2 \\ C_2 & D_2 \end{bmatrix} \quad (10)$$

$$\begin{bmatrix} A_8 & B_8 \\ C_8 & D_8 \end{bmatrix} = \begin{bmatrix} A_4 & B_4 \\ C_4 & D_4 \end{bmatrix} \cdot \begin{bmatrix} A_5 & B_5 \\ C_5 & D_5 \end{bmatrix} \cdot \begin{bmatrix} A_6 & B_6 \\ C_6 & D_6 \end{bmatrix} \quad (11)$$

$$\begin{bmatrix} A_9 & B_9 \\ C_9 & D_9 \end{bmatrix} = \begin{bmatrix} A_5 & B_5 \\ C_5 & D_5 \end{bmatrix} \cdot \begin{bmatrix} A_6 & B_6 \\ C_6 & D_6 \end{bmatrix} \quad (12)$$

APPENDIX B

The UGC electrical characteristics are the typical values for XLPE type cables with conductor cross-section of 2500 mm² for the EHV and 1600 mm² for the HV. The transformer leakage inductance is a typical value for transmission transformers used in the Netherlands. For the loading condition a relatively low load of 100 MW + 50 MVar was chosen and the resistance and inductance value are calculated for the series connected load.

TABLE I
NETWORK PARAMETERS FOR BASE CASE SCENARIO

	R	L	C
External grid	-	0.02 H	-
OHL	0.0126 Ω /km	0.7585 mH/km	0.0152 μ F/km
400 kV Cable	0.0695 Ω /km	0.2883 mH/km	0.2147 μ F/km
Transformer	-	0.217 H	-
150 kV Cable	0.1112 Ω /km	0.3790 mH/km	0.2423 μ F/km
Load	180 Ω	0.2865 H	-

REFERENCES

- [1] Working Group B1.30, Cigre: "Cable Systems Electrical Characteristics", April 2013.
- [2] B. Gustavsen: "Study of Transformer Resonant Overvoltages Caused by Cable-Transformer High-Frequency Interaction", IEEE Transactions on Power Delivery, vol. 25, No. 2, pp. 770 - 779, April 2010.
- [3] Working Group C4.502, Cigre: "Power System Technical Performance Issues Related to the Application of Long HVAC Cables", October 2013.
- [4] Tokyo Electric Power Company: "Assessment of the Technical Issues relating to Significant Amounts of EHV Underground Cable in the All-island Electricity Transmission System", November 2009.
- [5] Teruo Ohno: "Dynamic Study on the 400 kV 60 km Kyndbyvaerket-Asnaesvaerket Line", PhD Thesis, Aalborg University, 2012.
- [6] T. Ohno, C.L. Bak, A. Ametani, W. Wiechowski and T.K. Sørensen: "Derivation of Theoretical Formulas of the Frequency Component Contained in the Overvoltage Related to Long EHV Cables", IEEE Transactions on Power Delivery, vol. 27, No. 2, pp. 866 - 876, April 2012.
- [7] A.I. Chysochos, T.A. Papadopoulos, G.K. Papagiannis: "Rigorous calculation method for resonance frequencies in transmission line responses", IET Generation, Transmission & Distribution, vol. 9, Issue 8, pp. 767 - 778, May 2015.
- [8] Ch.G. Kaloudas, T.A. Papadopoulos, G.K. Papagiannis: "Spectrum analysis of transient responses of overhead transmission lines", UPEC 2010, Cardiff, Wales, 2010
- [9] Task Force on Harmonic Modeling and Simulation, "Impact of Aggregate Linear Load Modeling on Harmonic Analysis: A Comparison of Common Practice and Analytical Models", IEEE Transactions on Power Delivery, Vol. 18, No. 2, April 2003, pp. 625-630.
- [10] Lei Wu: "Impact of EHV/HV Underground Power Cables on Resonant Grid Behavior", PhD dissertation, Eindhoven University of Technology, 2014.
- [11] A. Morched, B. Gustavsen, M.Tartibi, "A universal model for accurate calculation of electromagnetic transients on overhead lines and underground cables," IEEE Transactions on Power Delivery, vol. 14, Issue: 3, pp. 1032-1038, Jul 1999.
- [12] Manitoba HVDC Research Centre Inc.: "EMTDC User's Guide", vol.4.7, fifth printing, February 2010.
- [13] Working Group 02, Cigre: "Guidelines for representation of network elements when calculating transients", 1985.
- [14] Wu, L., Fonk, H., Wouters, P.A.A.F., Steennis, E.F.: "Influence by parasitic capacitances on frequency response of a 380-150-50 kv transformer with shunt reactor", Int. Symposium on High Voltage Engineering (ISH), Seoul, August 2013.
- [15] IEEE Modeling and Analysis of System Transients Working Group: "Modeling Guidelines for Switching Transients", 1998.